Environmental Science & Technology

Article

pubs.acs.org/est

Electrochemical Transformation of Trace Organic Contaminants in the Presence of Halide and Carbonate Ions

James M. Barazesh, Carsten Prasse, and David L. Sedlak*

Department of Civil and Environmental, Engineering University of California, Berkeley, California 94720, United States

Supporting Information

ABSTRACT: Electrochemical treatment on anodes shows promise for the oxidation of organic contaminants in industrial wastewater and reverse osmosis concentrate from municipal wastewater recycling due to the high conductivity of the matrix and the concomitant low energy demand. The effect of background electrolyte composition (Cl^-, HCO_3^-, and NH_4^+) on the formation and fate of electrochemically produced heterogeneous ($HO^\bullet_{ads}$ and $Cl^\bullet_{ads}$) and homogeneous (HOCl and HOBr) oxidants was evaluated on Ti−IrO_2 and boron-doped diamond (BDD) electrodes using a suite of trace organic contaminants that exhibited varying reactivity with $HO^\bullet$, $CO_3^{\bullet-}$, HOCl, and HOBr. The contributions of adsorbed and bulk oxidants to contaminant degradation were investigated. Results show that transformation rates for most contaminants increased in the presence of chloride and trace amounts of bromide; however, elevated concentrations of HCO_3^- often altered transformation rates due to formation of selective oxidants, with decreases in reactivity observed for electron-poor contaminants and increases in reactivity observed for compounds with amine and phenolic moieties. Using this information, rates of reactions on anode surfaces and measured production and loss rates for reactive homogeneous species were used to predict contaminant removal in municipal wastewater effluent. Despite some uncertainty in the reaction mechanisms, the model accurately predicted rates of removal of electron-rich contaminants but underestimated the transformation rates of compounds that exhibited low reactivity with HOCl and HOBr, possibly due to the formation of halogen radicals. The approach employed in this study provides a means of identifying key reactions for different classes of contaminants and for predicting the conditions under which anodic treatment of wastewater will be practical.

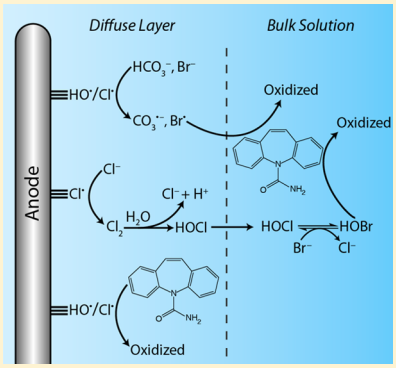

INTRODUCTION

Electrochemical treatment of contaminated groundwater, industrial wastewater, and hazardous waste has gained interest as an alternative to advanced oxidation processes due to its ease of operation and ability to degrade a wide range of organic contaminants.[1−4] In halide-free solutions, anodic treatment of contaminants proceeds through a combination of direct oxidation of compounds on the electrode surface and reaction with reactive species produced by partial oxidation of water. In particular, adsorbed hydroxyl radical ($HO^\bullet_{ads}$) has been invoked as an important oxidant generated at the surface of active electrodes.[1,5]

When anodic treatment is performed in wastewaters and brines containing an abundance of halide ions, the rate of disappearance of organic contaminants often increases due to the formation of halogen-containing oxidants in the bulk solution, such as Cl_2, HOCl, and Br_2.[4,6−8] Most researchers have ignored the possible role of adsorbed halogen species in contaminant transformation, despite their role as intermediates in the Volmer−Heyrovsky mechanism of electrochemical chlorine production:[9−13]

$$\equiv S + Cl^- \underset{k_{-1}}{\overset{k_1}{\longleftrightarrow}} \equiv S(Cl^\bullet_{ads}) + e^- \quad (1)$$

$$\equiv S(Cl^\bullet_{ads}) + Cl^- \overset{k_2}{\rightarrow} \equiv S + Cl_2 + e^- \quad (2)$$

where ≡S corresponds to a surface lattice oxygen group[14] that serves as the active site for the oxidation of chloride. Formation of adsorbed chlorine atom ($Cl^\bullet_{ads}$) occurs at a much lower potential than $HO^\bullet_{ads}$ and therefore can be a significant anodic process, especially at the potentials used in electrochemical water treatment.[9] Previously published data indicate that formation of Cl_2 (i.e., reaction 2) is limited by the rate of recombination of $Cl^\bullet_{ads}$ and the rate of diffusion of Cl_2 away from the electrode,[9,15] enabling an accumulation of $Cl^\bullet_{ads}$ on anode surfaces (e.g., surface densities of up to 1.2×10^{-8} mol cm^{-2} have been observed on RuO_2 electrodes).[13]

The importance of $Cl^\bullet_{ads}$ and other reactive halogens to contaminant transformation depends on their relative reactivity with halides and organic contaminants. In solution, chlorine atoms ($Cl^\bullet$) react with most organic contaminants at near-diffusion controlled rates (10^8−10^{10} M^{-1} s^{-1}).[16] However, other mechanisms of $Cl^\bullet_{ads}$ loss (e.g., recombination with $Cl^\bullet_{ads}$ to form Cl_2, propagation with Cl^- to form $Cl_2^{\bullet-}$, and reactions

Received: May 4, 2016
Revised: August 20, 2016
Accepted: August 24, 2016

DOI: 10.1021/acs.est.6b02232
Environ. Sci. Technol. XXXX, XXX, XXX−XXX

with other scavengers) may limit its role in contaminant transformation during electrochemical treatment. Nonetheless, there is evidence that $Cl^{\bullet}_{ads}$ formed via anodic oxidation may be important to contaminant transformation.[17] Although the exact nature of adsorbed radicals (e.g., $HO^{\bullet}_{ads}$ and $Cl^{\bullet}_{ads}$) is still unclear, it appears that they can play an important role in heterogeneous systems and that their reactivity toward contaminants differs from that of their homogeneous analogues.[2,5,18]

Electrochemical treatment of waters containing elevated concentrations of dissolved solutes (e.g., brackish groundwater, wastewater effluent, and reverse osmosis concentrate)[3,6−8] can be affected by the matrix composition. In particular, reactions involving natural organic matter (NOM), bromide, bicarbonate, and ammonium ions on the electrode surface can lead to the formation of selective solution-phase oxidants (e.g., $CO_3^{\bullet-}$ and $NH_2^{\bullet}$) that affect the rate of oxidation of certain trace organic compounds.[19−22] Information on the formation and fate of these species in electrochemical systems is still limited.

The objective of this study was to gain insight into the role of different oxidants in contaminant transformation when electrolysis is employed for treatment of organic contaminants in waters containing halides and other solutes typically present in natural waters and municipal wastewater. By evaluating the oxidation of organic contaminants in the presence of various inorganic constituents, better strategies can be developed for assessing conditions under which electrochemical treatment is appropriate. To provide insight into the importance of transient species generated during electrolysis, both adsorbed to the electrode surface and in the bulk solution, the fate of a suite of trace contaminants exhibiting varying reactivity with different species was evaluated on two representative anodes (i.e., Ti−IrO_2 and boron-doped diamond) used in electrochemical water treatment.

■ MATERIALS AND METHODS

Materials. All experiments were performed with reagent-grade $NaHCO_3$, NaCl, NaBr, NH_4Cl, and $Na_2B_4O_7$, and analytical reference standards of organic contaminants (Sigma-Aldrich, St. Louis, MO). Chemical structures of trace organic contaminants studied are included in Table S1. Stable-isotope-labeled analogues used as internal standards were obtained from Toronto Research Chemicals, Ontario, Canada. Suwannee River humic acid (SRHA) and Pony Lake fulvic acid (PLFA) were obtained from the International Humic Substances Society. Fluka analytical-grade NaCl (<0.001% Br^- by weight) was used for experiments performed with an electrolyte containing greater than 10 mM NaCl to minimize the possible effects of trace bromide impurities. NaOCl stock solutions were standardized monthly using *N*,*N*-diethyl-*p*-phenylenediamine (DPD) colorimetry.[23] Hypobromous acid (HOBr) stock solutions were prepared by adding 10% excess bromide to NaOCl solutions.[24] Grab samples of post-microfiltration wastewater effluent were obtained from the East Bay Municipal Utility District's wastewater treatment plant (Oakland, CA).

Reaction Rate Constants for Organic Contaminants and Oxidants. Pseudo-first-order rate constants for the reaction of test compounds with HOCl and HOBr were determined at pH 8.0 in 10 mM borate buffer. Solutions containing 10 μg L^{-1} of target compounds were amended with 0.1 to 1 mM NaOCl/NaOBr to initiate experiments, which were performed in triplicate. Samples were periodically collected, quenched with excess thiosulfate (3:1 thiosulfate-to-chlorine/bromine molar ratio), and analyzed for trace organic compounds.

Electrolysis Setup. Electrolysis experiments were carried out using either a Ti−IrO_2 mixed-metal oxide anode (64 cm^2; Magneto Special Anodes, Netherlands) or a BDD Diafilm EP anode (1.13 cm^2; Element 6; Spring, TX) in a single-chambered parallel plate electrochemical cell. In both cases, the anode was coupled with a stainless steel cathode of the same surface area (grade: 316L; Solana, Belgium; Figure S2). Electrolytes ($V_{TOT,Ti-IrO_2}$ = 250 mL; $V_{TOT,BDD}$ = 50 mL) were recirculated at a rate of 5 L h^{-1}. All experiments were performed at a fixed current of 80 A m^{-2} controlled by a multichannel potentiostat (Gamry Instruments Inc., Warminster, PA).

Electrolysis Experiments. Electrolysis experiments were conducted in a supporting electrolyte (10 mM borate buffer; pH 8.0 or 10.0) containing a mixture of 11 test compounds each at concentration of 10 μg L^{-1}. To elucidate the role of different solutes on transformation rates, the borate-buffered electrolyte was additionally modified with either NaCl, NH_4Cl, NaBr, $NaHCO_3$, or NOM. The pH was monitored over the course of the experiment and never changed by more than 0.1 unit. Samples were periodically collected, quenched with excess thiosulfate (3:1 thiosulfate-to-chlorine molar ratio), and analyzed for trace organic compounds within 12 h.

Experiments performed in the absence of current to assess sorption of contaminants to the anode indicated only modest losses of propranolol via adsorption ($k_{Ti-IrO_2} = 5.6 \times 10^{-4}$ s^{-1}). To assess the influence of reduction on the cathode to observed transformation rates, electrolysis of NaCl was performed in a dual-chambered electrochemical cell separated by a cation exchange membrane (Ultrex CMI-7000, Membranes International Inc., Ringwood, NJ). HOCl production and contaminant transformation rates were nearly identical when experiments were conducted with the anode chamber isolated from the system, indicating that cathodic reactions were unimportant to chlorine accumulation or contaminant transformation.

Cyclic voltammograms to determine the potentials required for direct oxidation of organic compounds were performed in a pH 8.0, 1.5 M $NaClO_4$ electrolyte at a scan rate of 10 mV s^{-1} over a 2 V potential range. Chronoamperometry experiments were performed to evaluate if inorganic solutes (e.g., HCO_3^- and Cl^-) underwent direct electron transfer on the anode. A potential of 1.55 V was applied using 0.5 M $NaClO_4$ at pH 8.0 until a stable current for water oxidation was reached.[25] At this point, the electrolyte was amended with 50 mM HCO_3^- or Cl^-, and the current increase was measured. High concentrations of solutes were used to prevent mass-transfer limitations at the anode surface.

Trace Organic Contaminant Removal via Electrolysis. Allyl alcohol (3-propenol, AA; 100 mM) or tertiary butanol (*t*-buOH; 100 mM) were used as selective quenchers to differentiate the importance of reactions involving adsorbed radicals (e.g., $Cl^{\bullet}_{ads}$ and $HO^{\bullet}_{ads}$) and dissolved radicals (e.g., $HO^{\bullet}$, $CO_3^{\bullet-}$) to contaminant electrolysis rates, respectively. Allyl alcohol was useful for probing surface-bound oxidants because the interaction of its π-orbitals with the positively charged anode surface and the high reactivity of the allylic carbon with oxidants allows it to react at the electrode surface.[26,27] In contrast, saturated alcohols (i.e., *t*-buOH) do not react readily with electrode surfaces,[28] yet react rapidly with dissolved oxidants ($HO^{\bullet}$ and $Cl^{\bullet}$; section 1.1.3 in the

DOI: 10.1021/acs.est.6b02232
Environ. Sci. Technol. XXXX, XXX, XXX−XXX

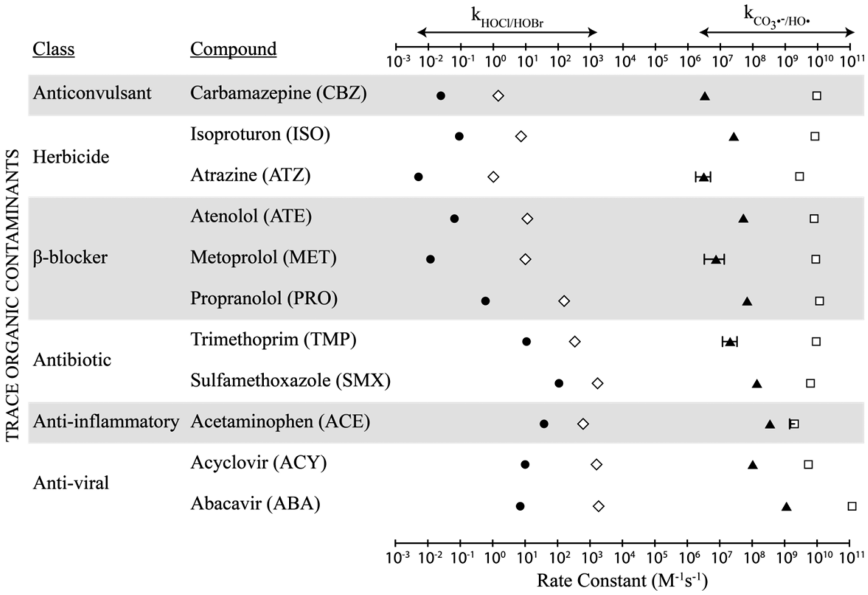

Figure 1. Bimolecular rate constants for the reaction between HOCl (●), HOBr (◇), $CO_3^{\bullet-}$ (▲), and $HO^\bullet$ (□) with trace organic contaminants. Rate constants for HOCl/HOBr were determined at pH 8.0. Error bars represent ± one standard deviation. In some cases, error bars are smaller than the data points. See Table S4 for data sources and values of second-order rate constants. See Table S1 for the chemical structures of the test compounds.

Supporting Information) and thus provide estimates of the importance of reactive solution-phase intermediates. Because allyl alcohol reacts rapidly with both heterogeneous and homogeneous oxidants, transformation of the contaminants observed in the presence of high concentrations of allyl alcohol were ascribed exclusively to direct electron transfer.

The bulk solution steady-state concentration of $HO^\bullet$ ($[HO^\bullet]_{SS}$) was measured using *para*-chlorobenzoic acid (*p*CBA; 10 μM) as a probe ($k_{pCBA,HO^\bullet} = 5 \times 10^9\ M^{-1}\ s^{-1}$).[29] Under the experimental conditions employed (i.e., $[Cl^-]$ = 10 mM; pH 8.0), $Cl^\bullet$ in the bulk solution was converted rapidly to $Cl_2^{\bullet-}$, which is relatively unreactive with *p*CBA ($k_{pCBA,Cl_2^{\bullet-}} = 3 \times 10^6\ M^{-1}\ s^{-1}$; section 1.1.1 in the Supporting Information).[30] Control experiments in the presence of allyl alcohol indicated that direct oxidation of adsorbed *p*CBA was negligible, which agreed with published literature.[31]

Due to accumulation of HOCl, the contribution of free chlorine to compound oxidation increased with time (section 1.3 in the Supporting Information).[8] This phenomenon was especially evident for compounds exhibiting high reactivity with HOCl (e.g., sulfamethoxazole, abacavir, acylovir, and trimethoprim). For these compounds, deviations from first-order disappearance ($0.95 < r^2 < 0.98$) were observed.

Quantification of Surface Titanol Group Density. The surface density of adsorbed oxidants is needed to determine if they are present at high enough concentrations to play a role in oxidation relative to their homogeneous analogues. Ion-exchange capacity provides a means of estimating active surface area of oxide electrodes.[32] The density of electrocatalytic sites for the formation of surface hydroxyl and chlorine radical (i.e., ≡TiOH)[10,15,33] was determined using the toluidine blue O (TBO) colorimetric method.[34] Briefly, electrodes were submerged in 0.05 mM TBO at pH 10.0 for 24 h at 30 °C to promote TBO adsorption to surface functional groups (i.e., $\equiv TiO^-$). Excess TBO was rinsed off with 1 M NaOH and adsorbed TBO was subsequently desorbed in 8 mL of 50% acetic acid. Samples were vortexed for 10 min prior to spectroscopic measurement at 633 nm.

Analytical Methods. Free chlorine and TBO concentrations were measured with a Shimadzu UV-2600 spectrophotometer using the DPD method at 515 nm[23] and the TBO method at 633 nm, respectively.[34] Test compounds were quantified by high-performance liquid chromatography–tandem mass spectrometry (HPLC–MS/MS) in the multiple reaction monitoring (MRM) mode using an Agilent 1200 series HPLC system with a Hydro-RP column (150 × 3 mm, 4uM; Phenomenex, Aschaffenburg, Germany) coupled to a 6460 triple quadrupole tandem mass spectrometer, as described previously.[35] *p*CBA was quantified on a high-performance liquid chromatography (HPLC) system equipped with UV detection at 254 nm (Agilent 1260 Infinity). Analytical details and compound specific parameters are provided in Table S2.

RESULTS AND DISCUSSION

Electrolysis rates for organic contaminants in the presence of halide and carbonate ions includes transformation via direct electron transfer in addition to contributions from reactive oxygen species ($HO^\bullet_{ads}$, $HO^\bullet$), reactive halide species ($Cl^\bullet_{ads}$, $Cl_2^{\bullet-}$, HOX), and $CO_3^{\bullet-}$.

Experiments performed with quencher compounds detailed in the Materials and Methods section were used to isolate reactive dissolved and adsorbed species and gain insight into their contribution to electrolysis rates.

Oxidation of Trace Organic Contaminants by Dissolved Oxidants. Reaction rates for the test compounds with HOCl and HOBr varied by more than 3 orders of magnitude, exhibiting faster kinetics for compounds containing electron-rich aniline and deprotonated amine moieties (Figure 1 and Table S4). Bimolecular rate constants for HOCl with test compounds were in good agreement with previously reported data (Table S5). Second-order reaction rate constants obtained from previous publications for trace organic contaminants with $HO^\bullet$ approached diffusion-controlled rates (10^9–$10^{11}\ M^{-1}$

DOI: 10.1021/acs.est.6b02232
Environ. Sci. Technol. XXXX, XXX, XXX−XXX

s^{-1}),[21,36−39] while rates of reaction with $CO_3^{\bullet-}$ ranged between 10^6 to 10^9 M^{-1} s^{-1},[21,37,40] reflecting the selectivity of $CO_3^{\bullet-}$ with the previously mentioned electron-rich structural moieties, such as the reactive cyclopropyl and amino-adenine moieties of abacavir and the guanine moiety present in acyclovir.[37]

Oxidation of Trace Organic Contaminants on Ti−IrO_2 Electrode Surfaces. HOCl production rates were fully inhibited by allyl alcohol (Figure S9; $k_{AA,\,Cl^\bullet} \approx 6 \times 10^8$ M^{-1} s^{-1}; section 1.1.2 in the Supporting Information) but were unaltered in the presence of *t*-buOH (Figure S9; $k_{t\text{-butanol},Cl^\bullet} = 1.5 \times 10^9$ M^{-1} s^{-1}),[41] thus confirming the selective reactivity of allyl alcohol with surface-bound oxidants (i.e., $Cl^\bullet_{ads}$). This was further supported by identical contaminant loss rates observed in borate, NaCl, and $NaHCO_3$ electrolytes in the presence of allyl alcohol, suggesting transformation was solely attributable to direct electron transfer from the anode to yield intermediate radical cations (Figure S3).[1] Cyclic voltammetry scans using acetaminophen as a probe compound indicated that oxidation via direct electron transfer of the adsorbed organics occurred at potentials above +0.75 V (Figure S23).

Impact of Solutes on Electrochemical Transformation of Contaminants. Observed loss rates for trace contaminants in borate buffer at pH 8.0 ranged from 3.4×10^{-5} to 7.3×10^{-3} s^{-1} (Figure 2 and Table S6). In general, the relatively slow rate of contaminant removal on Ti−IrO_2 can be attributed to the low $HO^\bullet_{ads}$ production at an anodic potential of ∼1.70 V at pH 8.0 (section 1.2 in the Supporting Information). Loss rates for the organic compounds were not affected by addition of *t*-buOH, indicating that contribution of dissolved $HO^\bullet$ (measured $[HO^\bullet]_{SS} = 3.2 \times 10^{-15}$ M) to overall compound loss was small relative to surface-bound oxidation processes (i.e., direct electron transfer and reactions with $HO^\bullet_{ads}$). The negligible importance of dissolved $HO^\bullet$ was consistent with the short lifetimes of the reactive radical (i.e., <1 μs) relative to the time needed for diffusion out of the boundary layer.[1,25]

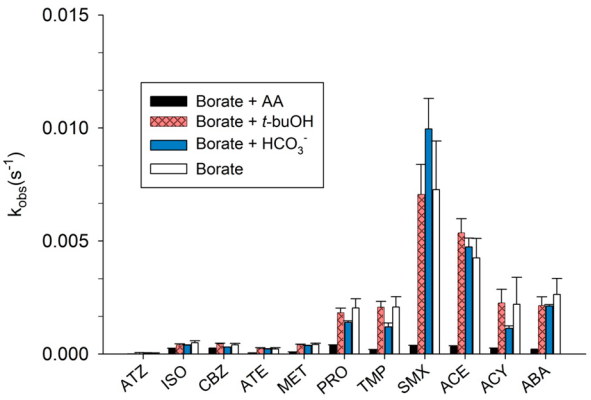

Figure 2. Observed first-order loss rates of trace organic contaminants on the Ti−IrO_2 electrode in 10 mM borate (pH 8.0) amended with 100 mM allyl alcohol (AA), 100 mM tertiary butanol (*t*-buOH), and 10 mM HCO_3^-. Error bars represent ± one standard deviation.

The very slow rate of removal of atrazine (ATZ) was attributed to the stability of the *s*-triazine ring to electrochemical oxidation, as shown in previous studies.[38,42−44] Similarly, the slow rate of loss of atenolol (ATE; pK_A 9.6) and metoprolol (MET; pK_A 9.1) at pH 8.0 was likely related to electrostatic repulsion between the positively charged anode surface and protonated amine functional groups. When the experiment was repeated at pH 10.0, the removal rate of atenolol and metoprolol increased by 330% and 190%, respectively (Figure S4).

Significantly reduced rates of removal of propranolol (PRO), trimethoprim (TMP), sulfamethoxazole (SMX), acetaminophen (ACE), acyclovir (ACY), and abacavir (ABA) in the presence of allyl alcohol indicated that $HO^\bullet_{ads}$ contributed greatly to transformation (>85%; Figure 2 and Table S9). In contrast, removal of isoproturon (ISO) and carbamazepine (CBZ) was only partially inhibited by allyl alcohol, suggesting that reactions with $HO^\bullet_{ads}$ are less important for these compounds (<45%). Differences in relative reactivities among structurally similar aromatic amides with small variations in electron density (e.g., ACE and ISO) implies that $HO^\bullet_{ads}$ is more selective than its dissolved counterpart. Unlike ISO, the phenolic functional group present in ACE was more susceptible to electrophilic attack by $HO^\bullet_{ads}$. The high reactivity of $HO^\bullet_{ads}$ with SMX can most likely be attributed to the electron-rich aniline and/or isoxazole moiety.

Effect of Chloride. The addition of 10 mM chloride dramatically enhanced the loss rates of all trace organic contaminants relative to those observed in the borate-buffered electrolyte (i.e., 4−20 times increase; Figure 3 and Table S7).

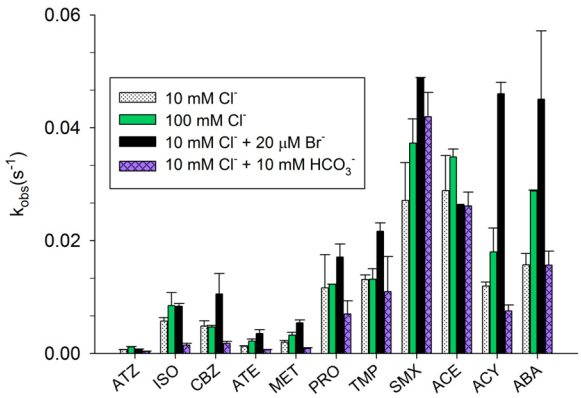

Figure 3. Observed first-order loss rates of trace organic contaminants on the Ti−IrO_2 electrode at pH 8.0 in 10 mM NaCl, 100 mM NaCl, 10 mM NaCl with 20 μM NaBr, and 10 mM NaCl with 10 mM HCO_3^-. Error bars represent ± one standard deviation.

Contaminant removal was not affected by the presence of *t*-buOH, suggesting that contribution of dissolved $HO^\bullet$ and $Cl_2^{\bullet-}$ to the transformation process was negligible (measured $[HO^\bullet]_{SS} = 1.3 \times 10^{-14}$ M; Figure S5; see section 1.1.3 in the Supporting Information). Compounds containing strong electron-donating moieties, such as deprotonated amines (TMP, ACY, and ABA), anilines (SMX), methoxy-naphthalenes (PRO), and phenolic groups (ACE), were removed faster due to rapid reactions with electrochemically generated HOCl (Figure 1). With the exception of abacavir and propranolol, estimates of transformation rates due to direct electron transfer, $HO^\bullet_{ads}$, and HOCl agreed to within 20% of observed values (Figure S27):

$$k_{pred} \approx k_{DET} + k_{HO^\bullet_{ads}} + k_{HOCl}[HOCl] \quad (3)$$

where k_{pred} is the predicted transformation rate (s^{-1}), k_{DET} and $k_{HO^\bullet ads}$ are the transformation rates (s^{-1}) due to direct electron transfer and surface-bound oxidants, respectively, (determined previously in borate buffered electrolyte in the presence and absence of allyl alcohol) and k_{HOCl} is the bimolecular rate constant of contaminants with HOCl (M^{-1} s^{-1}; SI Section 1.3).

DOI: 10.1021/acs.est.6b02232
Environ. Sci. Technol. XXXX, XXX, XXX−XXX

Use of eq 3 significantly underpredicted transformation rates for CBZ, MET, and ATZ, suggesting that reactive species other than $HO^{\bullet}_{ads}$ (<20%) or HOCl (<25%) were responsible for the increase in transformation rates upon addition of Cl^- (Table S10). For these compounds, differences in predicted and observed removal were ascribed to reaction with $Cl^{\bullet}_{ads}$, which accounted for the majority of the observed loss (i.e., > 50%; Table S10).

Estimates of the surface density of adsorbed chlorine atom can be made using the current efficiency for chlorine production with the total active surface hydroxyl group density (i.e., [≡TiOH]) on the Ti−IrO_2 electrode, which was determined to be $5.44 \pm 0.37 \times 10^{-8}$ moles cm^{-2}. This value agreed with reported surface densities of oxide electrocatalysts for similar types of mixed-metal oxide electrodes ($RuO_2 \approx 4 \times 10^{-8}$ moles cm^{-2}).[12,45] Given a 23% current efficiency in a 10 mM NaCl electrolyte, we estimate steady-state $Cl^{\bullet}_{ads}$ densities of 1.25×10^{-8} mol cm^{-2}, which agree with surface densities of 1.2×10^{-8} mol cm^{-2} determined with in situ thin-gap radiotracer methods using ^{36}Cl at similar chloride concentrations.[13]

Rates of removal of trace organic contaminants, with the exception of CBZ, increased between 16 to 160% as chloride concentrations increased from 10 to 100 mM (Figure 3). Faster removal rates can be explained by an increase in current efficiency for the two-electron transfer from Cl^- to Cl_2 (i.e., from 23% to 60%) as the chloride concentration was increased by an order of magnitude, resulting in greater chlorine atom surface density and a factor of 3 increase in HOCl production rates (Figure S10). The relatively small increases in HOCl production at higher chloride concentrations were attributable to mass-transfer limitations as well as an inversely proportional relationship between the rate-determining electrochemical desorption step of $Cl^{\bullet}_{ads}$ (i.e., k_2) and chloride concentration.[15] Removal rates decreased by 38−69% for the entire suite of trace organic contaminants at lower chloride concentrations characteristic of groundwater or surface water (i.e., ∼1 mM) due to low faradaic efficiency for chlorine evolution (<5%; data not shown).

Effect of Bromide. The addition of 20 μM Br^- to a 10 mM NaCl solution resulted in the increased removal rates for all of the trace organic contaminants (Figure 3). In this system, bromide rapidly reacted with hypochlorous acid to produce hypobromous acid (HOBr):[46]

$$HOCl + Br^- \xrightarrow{k = 1.6-2.95 \times 10^3\ M^{-1}s^{-1}} HOBr + Cl^- \quad (4)$$

Given that reaction 3 is fast compared to the rate of oxidation of contaminants, and considering the rapid rate of HOCl production (i.e., HOCl is in excess), it is likely that essentially all of the Br^- was converted to HOBr within seconds of the initiation of electrolysis (i.e., $[HOBr] \approx [Br^-] = 20$ μM).[24] The observed transformation rates for compounds containing strong electron-donating moieties agreed well with predicted removal rates estimated by considering only the contribution of HOX to oxidation (i.e., $k_{obs} \approx k_{HOCl}[HOCl] + k_{HOBr}[HOBr]$; section 1.3 and Figure S28 in the Supporting Information). Because k_{HOBr} values were much greater than k_{HOCl} values (Figure 1 and Table S4), the presence of trace concentrations of Br^- increased the rate of removal of the organic contaminants (+10% to +285%) despite HOBr only accounting for a small portion of the total HOX. Notably, removal rates of contaminants in 10 mM NaCl with 20 μM NaBr were faster than those observed in 100 mM NaCl (Figure 3), suggesting that trace HOBr will displace HOCl as the most important HOX species in reverse osmosis concentrate from municipal wastewater, which typically contains over 40 μM Br^-,[8,47] and brines from shale gas production (>100 μM Br^-).[48]

Again, transformation rates for ATZ, ISO, CBZ, ATE, and MET increased slightly despite being relatively unreactive with HOX (i.e., $k_{HOCl}[HOCl] + k_{HOBr}[HOBr] \ll k_{obs}$). Experiments conducted in borate amended with 20 μM NaBr showed negligible HOX production (<1 μM detection limit); however, removal rates were similar to those observed in the 10 mM NaCl−20 μM Br^- electrolyte ([HOBr ≈ 20 μM]; Figure S14). Results suggest that for less-reactive compounds (i.e., $k_{HOBr} < 10\ M^{-1}\ s^{-1}$), surface-bound reactive bromine species (i.e., $Br^{\bullet}_{ads}$) possibly contributed to oxidation.[49,50]

Effect of Bicarbonate. The addition of 10 mM HCO_3^- decreased the loss rates of ATZ, ISO, CBZ, ATE, and MET by approximately 50 to 75% relative to removal rates in 10 mM NaCl (Figure 3). Although adsorption of anions with a stronger affinity for electrode surface functional sites, such as sulfate and phosphate, slows the rate formation of HOCl,[15] HOCl accumulation rates only decreased by approximately 25% in the presence of 10 mM HCO_3^- (Figure S15). The blockage of oxidation sites by adsorbed HCO_3^- was ruled out as the mechanism for the observed decreased transformation rates of the former compounds because the transformation rates of HOCl-reactive ABA, ACY, ACE, and SMX showed negligible or slightly increased removal when HCO_3^- was increased to 50 mM despite an approximately 85% decrease in chlorine production (Figure S15). The variability in transformation rates in the presence of HCO_3^- was likely attributable to the scavenging of $Cl^{\bullet}_{ads}$ by HCO_3^-:

$$Cl^{\bullet}_{ads} + HCO_3^- \xrightarrow{k_{homogenous} = 2.2 \times 10^8\ M^{-1}s^{-1}} Cl^- + H^+ + CO_3^{\bullet -} \quad (5)$$

$CO_3^{\bullet -}$ reacts slowly with ATZ, ISO, CBZ, ATE, and MET (Figure 1 and Table S4). The effect of HCO_3^- on the rate of transformation of ABA, ACY, ACE, and SMX was negligible due to the high reactivity of these compounds with $CO_3^{\bullet -}$. Unlike the situation in the NaCl electrolyte, decreases in removal rates after addition of *t*-buOH to the carbonate-containing electrolyte confirmed a shift from adsorbed oxidants to dissolved oxidants (i.e., $CO_3^{\bullet -}$; $k_{CO_3^{\bullet -},t\text{-buOH}} = 1.6 \times 10^2\ M^{-1}\ s^{-1}$; Figure S6).[30] Results from chronoamperometric experiments did not indicate a current increase upon the addition of HCO_3^- to an inert supporting electrolyte, suggesting that $CO_3^{\bullet -}$ was not formed through direct electron transfer on the anode (Figure S16).[25] Experiments conducted in borate-buffered electrolyte with and without 10 mM HCO_3^- did not show a similar effect of HCO_3^- on the removal of contaminants observed in the NaCl electrolyte, plausibly due to the lower reactivity of HCO_3^- with $HO^{\bullet}$ compared to that with $Cl^{\bullet}$ ($k_{HCO_3^-,HO^{\bullet}} = 8.5 \times 10^6\ M^{-1}\ s^{-1}$; Figure 2).

Further insight into $CO_3^{\bullet -}$ formation as a scavenging mechanism for adsorbed halide radicals can be obtained by observing the effect of HCO_3^- on contaminant transformation rates in the 10 mM NaCl−20 μM NaBr matrix. Linear correlations were observed between the carbonate radical rate constant (i.e., $k_{CO_3^{\bullet -}}$) and the change in pseudo-first-order removal rates when 10 mM HCO_3^- was amended to a 10 mM NaCl electrolyte ($r^2 = 0.41$; Figure S17) and to a 10 mM

DOI: 10.1021/acs.est.6b02232
Environ. Sci. Technol. XXXX, XXX, XXX−XXX

NaCl−20 μM NaBr electrolyte (r^2 = 0.63; Figure S18). These results indicate that despite the previously observed improvement in efficacy from the electrolysis of halide ions, the efficiency of the treatment is compound-specific when performed in the presence of moderate amounts of bicarbonate due to formation of more selective oxidants (Figure 4).

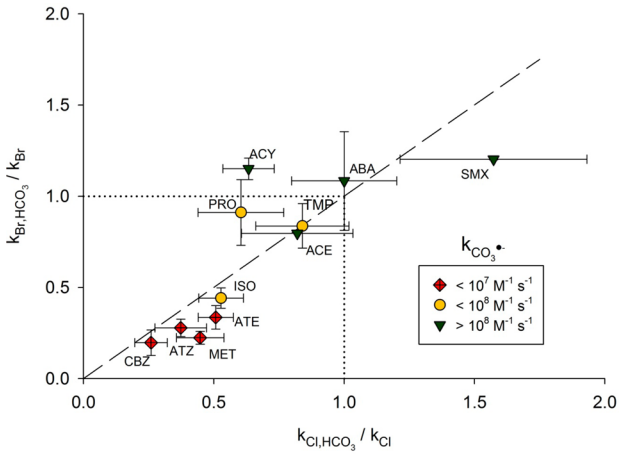

Figure 4. Relationship between the changes in pseudo-first-order degradation rates when 10 mM HCO_3^- was added to a 10 mM NaCl electrolyte ($k_{Cl,HCO3}/k_{Cl}$; x-axis) and to a 10 mM NaCl−20 μM NaBr electrolyte ($k_{Br,HCO3}/k_{Br}$; y-axis) on a Ti−IrO_2 electrode at pH 8.0. Error bars represent ± one standard deviation.

Consequently, electrolysis of electron-rich organic contaminants with $k_{CO_3^{\bullet-}}$ greater than 10^8 M^{-1} s^{-1} (e.g., sulfonamides,[21] antiviral nucleoside analogs)[37] will require similar or less electrolysis time than in the absence of HCO_3^-. Conversely, electron-poor compounds that react with $CO_3^{\bullet-}$ at rates below 10^7 M^{-1} s^{-1} (e.g., β-blockers[21] and triazine herbicides[40]) have reduced rates of transformation and will require slightly longer treatment times for adequate compound removal in the presence of HCO_3^-.

Effect of Ammonia. In the presence of ammonia, the rate of transformation of TMP, SMX, and ACE decreased due to the formation of combined chlorine (i.e., NH_2Cl), which is less reactive with these compounds than HOCl (Figure S19).[51−53] The removal rates of the remaining compounds (k_{HOCl} < 10 M^{-1} s^{-1}) were unchanged or increased slightly in the presence of ammonia. Partial inhibition of transformation rates in the presence of t-buOH indicated a shift from adsorbed to dissolved oxidants (Figure S19). The enhanced rate of transformation observed in the presence of ammonia for some compounds may have been attributable to the formation of reactive nitrogen species (e.g., $NH_2^\bullet$, $NO^\bullet$, and $NO_2^\bullet$) from the reaction of NH_3/NH_4^+ with $HO^\bullet$ ($k_{NH_3,HO^\bullet}$ = 1.0 × 10^8 M^{-1} s^{-1})[54,55] or $Cl^\bullet$.[14,33] The aminoperoxy radical ($NH_2O_2^\bullet$, ε_{350} ≈ 700 M^{-1} cm^{-1})[56] formed from the reaction between $NH_2^\bullet$ and O_2 in 1 M NH_3 was detected spectroscopically in both a UV−H_2O_2 control and 10 mM Cl^- electrolysis experiments at pH 8.0 and 10.5 (Figure S21). Furthermore, formation of NO_2^-/NO_3^- was observed, which is consistent with $NH_2^\bullet$ oxidation to $NH_2O_2^-$ and decomposition in solution (Figure S22).[54]

Significant increases in the removal rates for the β-blockers (+85−370%) is consistent with the modest reactivity of $NH_2^\bullet$ with secondary amines (10^4−10^5 M^{-1} s^{-1}).[57] The observed increase in transformation rates of contaminants containing weakly electron-donating moieties (CBZ, MET, ATE, and ATZ) in NH_4Cl relative to NaCl was absent upon addition of NOM (5 mgC L^{-1}), highlighting the plausible contribution of dissolved secondary reactive nitrogen species ($k_{NH_2^\bullet,NOM}$ = 1 L mgC^{-1} s^{-1}) to oxidation (Figure S20).[57] These findings suggest that reactive nitrogen species will not play an important role in the removal of these compounds during the treatment of natural waters.

Effect of Natural Organic Matter. Reaction of HOCl with SRHA (5 mgC L^{-1}) decreased HOCl evolution with increasing electrolysis time (−22%; Figure 5A). The absence of significant

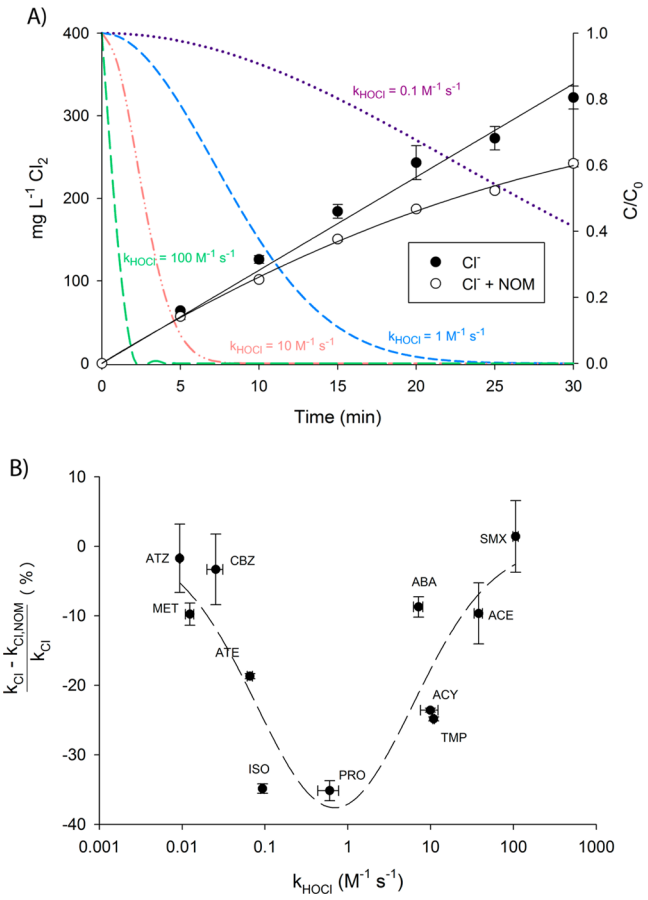

Figure 5. (A) Residual HOCl as a function of time in the presence and absence of 5 mg L^{-1} Suwannee River humic acids on Ti−IrO_2 during electrolysis of a 10 mM NaCl electrolyte (left axis). Modeled losses of organic contaminants exhibiting varying reactivity with HOCl (right axis). (B) Percent reduction of removal rates of trace organic contaminants in a pH 8.0, 10 mM NaCl electrolyte when amended with 5 mgC L^{-1} SRHA on Ti−IrO_2. Dashed lines show the fitted log-normal distribution (r^2 = 0.71). Error bars represent ± one standard deviation.

differences in HOCl concentration at short electrolysis times indicated that NOM competition with chloride for direct electrolysis sites and interaction with adsorbed oxidants was negligible (section 1.5 in the Supporting Information). Accordingly, compounds transformed primarily through reactions with surface-bound oxidants (e.g., CBZ, MET, and ATZ) were unaffected by the presence of NOM (Figure 5B).

An absence of inhibitory effects of humic substances on transformation rates for compounds exhibiting rapid kinetics with HOCl (k_{HOCl} > 10 M^{-1} s^{-1}; SMX, ABA, and ACE) was

DOI: 10.1021/acs.est.6b02232
Environ. Sci. Technol. XXXX, XXX, XXX−XXX

consistent with their elimination prior to significant loss of HOCl by reactions with phenolic, quinone, and amine moieties present in NOM (Figure 5A). Compounds exhibiting intermediate reactivity with HOCl (k_{HOCl} = 0.1−10 M^{-1} s^{-1}; PRO, TMP, ACY, and ISO) exhibited up to 40% slower removal rates in the presence of NOM. Comparable transformation rates using less-aromatic Pony Lake fulvic acid precluded the role of inhibition from reversion of partially oxidized compounds to parent compounds via reactions with antioxidant moieties present in NOM (Figure S24).[58−60]

Impact of Anode Material on Electrochemical Transformation of Contaminants. Different electrode materials exhibit wide variations in their ability to oxidize water to hydroxyl radicals (i.e., the O_2 overpotential varies) as well as the nature of the interaction between the adsorbed radicals and the electrode surface.[1,2] For example, BDD electrodes tend to be better-suited for contaminant degradation than Ti−IrO_2 in the absence of chloride due to their ability to produce higher yields of weakly adsorbed $HO^{\bullet}$.[5] Significant increases were observed in surface-area normalized removal rates (100−2500%) on BDD relative to Ti−IrO_2 in borate-buffered electrolyte, consistent with a higher production of $HO^{\bullet}$ (ϕ_{anode} = 4.0 V versus SHE, measured $[HO^{\bullet}]_{SS}$ = 2.8 × 10^{-14} M; Figure S7). Consequently, transformation rates decreased (∼85%) to rates of direct electrolysis upon addition of *t*-buOH. Partial inhibition (57 ± 15%) of both contaminant oxidation rates and $[HO^{\bullet}]_{SS}$ occurred during the electrolysis of borate in the presence of SRHA. Steady-state $HO^{\bullet}$ concentration in the presence of SRHA was roughly 2 orders of magnitude greater than expected ($k_{HO^{\bullet},SRHA}$ = 5.7 × 10^8 L M_C^{-1} s^{-1}; section 1.1.4 in the Supporting Information),[61] plausibly due to the slow diffusion of high-molecular weight NOM into the reactive zone adjacent to the electrode.[57]

The presence of chloride increased contaminant removal rates (Figure S8 and Table S8), although lower current efficiency was measured for Cl_2 production (7.8%) on BDD relative to Ti−IrO_2. Inhibition of HOCl production in the presence of *t*-buOH suggests that the formation pathway involves dissolved species,[62] and thus, the applicability of *t*-buOH to elucidate respective oxidation pathways (i.e., reactive radicals from HOX) is limited. Nonetheless, the dissolved oxidants (e.g., $HO^{\bullet}$,$Cl_2^{\bullet-}$, and HOCl) contributed significantly to contaminant transformation, as evidenced by a 20−98% reduction in electrolysis rates observed in the presence of *t*-buOH (Figure S8). Interestingly, the absence of a strong effect of NOM on HOCl production despite the importance of dissolved oxidants in this system suggests that the interaction of reactive halide species (i.e., $Cl^{\bullet}$ and $Cl_2^{\bullet-}$) with NOM is slow (Figure S12).[19,21,63] This was consistent with minimal effects of NOM on the transformation rates of electron-poor contaminants during electrolysis (Figure S25) and UV photolysis (Figure S26 and section 1.4 in the Supporting Information) in the presence of halides. Similar to Ti−IrO_2, the removal of compounds with bimolecular rate constants for reaction with $CO_3^{\bullet-}$ below 10^6 M^{-1} s^{-1} (e.g., CBZ and ATZ) was inhibited when the chloride electrolyte was amended with carbonate (data not shown).

Removal of Trace Organic Contaminants from Municipal Wastewater Effluent. To gain insight into the potential for using anodes to transform contaminants under realistic operating conditions, an experiment was conducted in 0.45 μm filtered municipal wastewater ([Cl^-] = 6.6 mM; [Br^-] = 7 μM; [NOM] = 9.5 mgC L^{-1}; see Table S3 for full composition) with the Ti−IrO_2 anode (Figure 6). Predicted removal rates for contaminants included contributions from

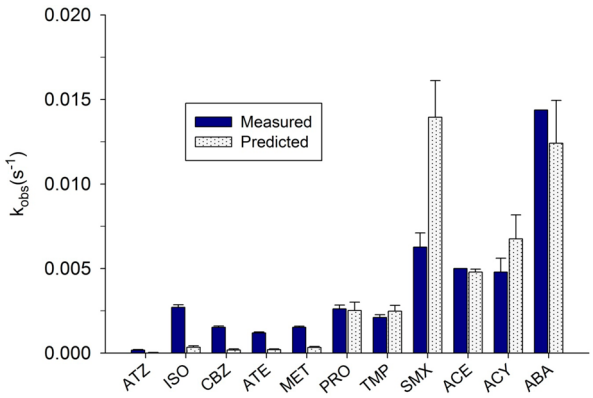

Figure 6. Predicted and measured pseudo-first-order removal rates for test compounds in pH 8.0 buffered municipal wastewater effluent on a Ti−IrO_2 electrode. Error bars represent ± one standard deviation.

direct electron transfer, dissolved $HO^{\bullet}$, $CO_3^{\bullet-}$, and reactions with dissolved HOCl and HOBr (section 1.3 in the Supporting Information). Due to the inability to quantify $[CO_3^{\bullet-}]_{SS}$ with probe compounds (i.e., *N*,*N*-dimethylaniline)[21,30,64] in the presence of HOCl,[65] the influence of $CO_3^{\bullet-}$ on removal rates was estimated by correcting the predicted contributions from direct electron transfer, $HO^{\bullet}$, HOCl, and HOBr with compound-specific scaling factors determined in Figure 4 (i.e., $k_{Br,HCO_3}/k_{Br}$). The contribution of $Cl^{\bullet}_{ads}$ was excluded from the model due to the absence of reliable estimates of bimolecular rate constants for organic compounds with $Cl^{\bullet}_{ads}$. Therefore, the underprediction of contaminant removal rates may be attributable to the contribution of $Cl^{\bullet}_{ads}$ and related halogen radical species.

In the municipal wastewater effluent, the rate of production of HOCl was slower than that observed in 10 mM NaCl due to the formation of chloramines ([NH_2Cl] = 0.26 mM), as well as slight inhibition in production due to the presence of NOM (9.5 mgC L^{-1}; Figure S13). The formation of combined chlorine did not increase contaminant removal rates due to its low reactivity with organic compounds ($k_{NH_2Cl,organics}$ < 0.05 M^{-1} s^{-1}).[51−53]

As expected, transformation rates were significantly underpredicted for those compounds that were less-reactive with HOCl and HOBr (i.e., k_{HOCl} < 1 M^{-1} s^{-1}) due to unaccounted for contributions from $Cl^{\bullet}_{ads}$ and $Br^{\bullet}_{ads}$. Predicted rates agreed well for compounds that exhibited high reactivity with HOCl/HOBr (PRO, TMP, ACY, and ABA) with the exception of SMX, which was removed at a slower rate than predicted by the combination of direct electron transfer and reactions with HOX. In the absence of NH_3, the predicted transformation rate agreed within 5% of the observed rate of SMX removal (Figure S27). The discrepancy between measured and predicted transformation rates highlights the need to consider the effects of additional solutes like NH_4^+ and SO_4^{2-} on oxidants, especially for electron-poor contaminants.

Environmental Implications. The efficiency with which contaminants are transformed on anodes depends upon the composition of the matrix and the nature of the anode. Higher salinity matrices, such as reverse osmosis concentrate from municipal wastewater and industrial wastewaters, are well-

DOI: 10.1021/acs.est.6b02232
Environ. Sci. Technol. XXXX, XXX, XXX−XXX

suited for electrochemical treatment due to the lower energy demand in conductive matrices. For these waters, faster removal rates will be observed for many compounds due to the presence of Cl^- and Br^-. For compounds that do not react quickly with HOCl or HOBr, removal may be hampered by the presence of HCO_3^-, which can scavenge reactive species like $Cl^\bullet$ and reduce the rate of transformation of prevalent electron-poor contaminants such as β-blockers[66] and triazine herbicides.[67] The predominance of reactions occurring on the electrode for contaminants containing weakly donating moieties suggest benefits of designing treatment systems with high surface area per volume of water treated. Optimization of the treatment of wastewater effluent and reverse osmosis concentrate may require the removal of NH_4^+ and NOM.

In addition to electrogenerated oxidants, toxic inorganic ions (e.g., chlorate, perchlorate, and bromate)[68] and halogenated transformation products may be formed on all types of anodes.[2,69] The concentration of these contaminants depends upon the nature of the electrode, solution composition, and the applied current. As this could limit the application of the technology, additional research is needed to develop tools to balance the benefits of efficient contaminant removal with the risks associated with formation of toxic byproducts.

■ ASSOCIATED CONTENT

Supporting Information

The Supporting Information is available free of charge on the ACS Publications website at DOI: 10.1021/acs.est.6b02232.

Additional details, 28 figures, and 10 tables with information on the electrolysis setup, chemical structures of test compounds, compound-specific mass spectrometry parameters, contribution of different oxidants to contaminant removal, measurements of rate constants for reactions of contaminants with HOCl, HOBr, and $Cl^\bullet$, and electroanalytical experiments (PDF)

■ AUTHOR INFORMATION

Corresponding Author

*E-mail: sedlak@berkeley.edu.

Notes

The authors declare no competing financial interest.

■ ACKNOWLEDGMENTS

This study was supported by the U.S. National Institute for Environmental Health Sciences (NIEHS) Superfund Research Program (grant no. P42 ES004705) and the Superfund Research Center at University of California, Berkeley. The authors thank Caroline Delaire and Dr. Jessica Ray for their insightful comments as well as Dr. Eva Agus for her help sampling wastewater effluent at the East Bay Municipal Utility District.

■ REFERENCES

(1) Chaplin, B. P. Critical review of electrochemical advanced oxidation processes for water treatment applications. *Environmental Science-Processes & Impacts* **2014**, *16* (6), 1182−1203.

(2) Radjenovic, J.; Sedlak, D. L. Challenges and Opportunities for Electrochemical Processes as Next-Generation Technologies for the Treatment of Contaminated Water. *Environ. Sci. Technol.* **2015**, *49* (19), 11292−11302.

(3) Bagastyo, A. Y.; Radjenovic, J.; Mu, Y.; Rozendal, R. A.; Batstone, D. J.; Rabaey, K. Electrochemical oxidation of reverse osmosis concentrate on mixed metal oxide (MMO) titanium coated electrodes. *Water Res.* **2011**, *45* (16), 4951−4959.

(4) Butkovskyi, A.; Jeremiasse, A. W.; Leal, L. H.; van der Zande, T.; Rijnaarts, H.; Zeeman, G. Electrochemical conversion of micropollutants in gray water. *Environ. Sci. Technol.* **2014**, *48* (3), 1893−1901.

(5) Comninellis, C. Electrocatalysis in the electrochemical conversion/combustion of organic pollutants for wastewater treatment. *Electrochim. Acta* **1994**, *39* (11−12), 1857−1862.

(6) Bagastyo, A. Y.; Batstone, D. J.; Rabaey, K.; Radjenovic, J. Electrochemical oxidation of electrodialysed reverse osmosis concentrate on Ti/Pt-IrO2, Ti/SnO_2-Sb and boron-doped diamond electrodes. *Water Res.* **2013**, *47* (1), 242−250.

(7) Eversloh, C. L.; Henning, N.; Schulz, M.; Ternes, T. A. Electrochemical treatment of iopromide under conditions of reverse osmosis concentrates - Elucidation of the degradation pathway. *Water Res.* **2014**, *48*, 237−246.

(8) Eversloh, C. L.; Schulz, M.; Wagner, M.; Ternes, T. A. Electrochemical oxidation of tramadol in low-salinity reverse osmosis concentrates using boron-doped diamond anodes. *Water Res.* **2015**, *72*, 293−304.

(9) Consonni, V.; Trasatti, S.; Pollak, F.; O'Grady, W. E. Mechanism of chlorine evolution on oxide anodes - study of pH effects. *J. Electroanal. Chem. Interfacial Electrochem.* **1987**, *228* (1−2), 393−406.

(10) Erenburg, R. G. Mechanism of the chlorine reaction of Ruthenium-Titanium oxide anodes. *Soviet Electrochemistry* **1984**, *20* (12), 1481−1486.

(11) Krishtalik, L. I. Kinetics and mechanism of anodic chlorine and oxygen evolution reactions on transition-metal oxide electrodes. *Electrochim. Acta* **1981**, *26* (3), 329−337.

(12) Ferro, S.; De Battisti, A. Electrocatalysis and Chlorine Evolution Reaction at Ruthenium Dioxide Deposited on Conductive Diamond. *J. Phys. Chem. B* **2002**, *106* (9), 2249−2254.

(13) Tomcsányi, L.; De Battisti, A.; Hirschberg, G.; Varga, K.; Liszi, J. The study of the electrooxidation of chloride at RuO2/TiO2 electrode using CV and radiotracer techniques and evaluating by electrochemical kinetic simulation methods. *Electrochim. Acta* **1999**, *44* (14), 2463−2472.

(14) Cho, K.; Qu, Y.; Kwon, D.; Zhang, H.; Cid, C. A.; Aryanfar, A.; Hoffmann, M. R. Effects of Anodic Potential and Chloride Ion on Overall Reactivity in Electrochemical Reactors Designed for Solar-Powered Wastewater Treatment. *Environ. Sci. Technol.* **2014**, *48* (4), 2377−2384.

(15) Trasatti, S. Progress in the understanding of the mechanism of chlorine evolution at oxide electrodes. *Electrochim. Acta* **1987**, *32* (3), 369−382.

(16) Buxton, G. V.; Bydder, M.; Salmon, G. A.; Williams, J. E. The reactivity of chlorine atoms in aqueous solution. Part III. The reactions of Cl-center dot with solutes. *Phys. Chem. Chem. Phys.* **2000**, *2* (2), 237−245.

(17) Park, H.; Vecitis, C. D.; Hoffmann, M. R. Electrochemical Water Splitting Coupled with Organic Compound Oxidation: The Role of Active Chlorine Species. *J. Phys. Chem. C* **2009**, *113* (18), 7935−7945.

(18) Tojo, S.; Tachikawa, T.; Fujitsuka, M.; Majima, T. Oxidation processes of aromatic sulfides by hydroxyl radicals in colloidal solution of TiO2 during pulse radiolysis. *Chem. Phys. Lett.* **2004**, *384* (4−6), 312−316.

(19) Grebel, J. E.; Pignatello, J. J.; Mitch, W. A. Effect of Halide Ions and Carbonates on Organic Contaminant Degradation by Hydroxyl Radical-Based Advanced Oxidation Processes in Saline Waters. *Environ. Sci. Technol.* **2010**, *44* (17), 6822−6828.

(20) Kiwi, J.; Lopez, A.; Nadtochenko, V. Mechanism and kinetics of the OH-radical intervention during fenton oxidation in the presence of a significant amount of radical scavenger (Cl-). *Environ. Sci. Technol.* **2000**, *34* (11), 2162−2168.

(21) Jasper, J. T.; Sedlak, D. L. Phototransformation of Wastewater-Derived Trace Organic Contaminants in Open-Water Unit Process Treatment Wetlands. *Environ. Sci. Technol.* **2013**, *47* (19), 10781−10790.

DOI: 10.1021/acs.est.6b02232
Environ. Sci. Technol. XXXX, XXX, XXX−XXX

(22) Rosario-Ortiz, F. L.; Wert, E. C.; Snyder, S. A. Evaluation of UV/H_2O_2 treatment for the oxidation of pharmaceuticals in wastewater. *Water Res.* **2010**, *44* (5), 1440−1448.
(23) American Public Health Association; American Water Works Association; Water Environment Federation. *Standard Methods for the Examination of Water and Wastewater*; Eaton, A. D.; Clesceri, L. S.; Greenberg, A. E.; Franson, M. A. H., Eds.; American Public Health Association: Washington, DC, 1998.
(24) Allard, S.; Fouche, L.; Dick, J.; Heitz, A.; von Gunten, U. Oxidation of Manganese(II) during Chlorination: Role of Bromide. *Environ. Sci. Technol.* **2013**, *47* (15), 8716−8723.
(25) Azizi, O.; Hubler, D.; Schrader, G.; Farrell, J.; Chaplin, B. P. Mechanism of Perchlorate Formation on Boron-Doped Diamond Film Anodes. *Environ. Sci. Technol.* **2011**, *45* (24), 10582−10590.
(26) Pastor, E.; Schmidt, V. M.; Iwasita, T.; Arevalo, M. C.; Gonzalez, S.; Arvia, A. J. The reactivity of primary C3-alcohols on gold electrodes in acid-media - a comparative-study based on DEMS data. *Electrochim. Acta* **1993**, *38* (10), 1337−1344.
(27) Celdran, R.; Gonzalezvelasco, J. J. Oxidation mechanism of allyl alcohol on an Au-electrode in basic solutions. *Electrochim. Acta* **1981**, *26* (4), 525−533.
(28) Solomon, J. L.; Madix, R. J. Kinetics and mechanism of the oxidation of allyl alcohol on Ag(110). *J. Phys. Chem.* **1987**, *91* (24), 6241−6244.
(29) Buxton, G. V.; Greenstock, C. L.; Helman, W. P.; Ross, A. B. Critical review of the rate constants for reactions of hydrated electrons, hydrogen-atoms, and hydroxyl radicals (.OH/.O-) in aqueous solution. *J. Phys. Chem. Ref. Data* **1988**, *17* (2), 513−886.
(30) Notre Dame Radiation Laboratory. Radiation Chemistry Data Center, Kinetics Database. https://www3.nd.edu/~ndrlrcdc/.
(31) Wang, H. J.; Bakheet, B.; Yuan, S.; Li, X.; Yu, G.; Murayama, S.; Wang, Y. J. Kinetics and energy efficiency for the degradation of 1,4-dioxane by electro-peroxone process. *J. Hazard. Mater.* **2015**, *294*, 90−98.
(32) Trasatti, S.; Petrii, O. A. Real surface area measurements in electrochemistry. *Pure Appl. Chem.* **1991**, *63* (5), 711−734.
(33) Cho, K.; Hoffmann, M. R. Urea Degradation by Electrochemically Generated Reactive Chlorine Species: Products and Reaction Pathways. *Environ. Sci. Technol.* **2014**, *48* (19), 11504−11511.
(34) Ray, J. R.; Lee, B.; Baltrusaitis, J.; Jun, Y.-S. Formation of Iron(III) (Hydr)oxides on Polyaspartate- and Alginate-Coated Substrates: Effects of Coating Hydrophilicity and Functional Group. *Environ. Sci. Technol.* **2012**, *46* (24), 13167−13175.
(35) Jasper, J. T.; Jones, Z. L.; Sharp, J. O.; Sedlak, D. L. Biotransformation of trace organic contaminants in open-water unit process treatment wetlands. *Environ. Sci. Technol.* **2014**, *48* (9), 5136−5144.
(36) De Laurentiis, E.; Prasse, C.; Ternes, T. A.; Minella, M.; Maurino, V.; Minero, C.; Sarakha, M.; Brigante, M.; Vione, D. Assessing the photochemical transformation pathways of acetaminophen relevant to surface waters: Transformation kinetics, intermediates, and modelling. *Water Res.* **2014**, *53*, 235−248.
(37) Prasse, C.; Wenk, J.; Jasper, J. T.; Ternes, T. A.; Sedlak, D. L. Co-occurrence of Photochemical and Microbiological Transformation Processes in Open-Water Unit Process Wetlands. *Environ. Sci. Technol.* **2015**, *49* (24), 14136−14145.
(38) Acero, J. L.; Stemmler, K.; Von Gunten, U. Degradation kinetics of atrazine and its degradation products with ozone and OH radicals: A predictive tool for drinking water treatment. *Environ. Sci. Technol.* **2000**, *34* (4), 591−597.
(39) Huber, M. M.; Canonica, S.; Park, G.-Y.; von Gunten, U. Oxidation of Pharmaceuticals during Ozonation and Advanced Oxidation Processes. *Environ. Sci. Technol.* **2003**, *37* (5), 1016−1024.
(40) Canonica, S.; Kohn, T.; Mac, M.; Real, F. J.; Wirz, J.; von Gunten, U. Photosensitizer Method to Determine Rate Constants for the Reaction of Carbonate Radical with Organic Compounds. *Environ. Sci. Technol.* **2005**, *39* (23), 9182−9188.
(41) Gilbert, B. C.; Stell, J. K.; Peet, W. J.; Radford, K. J. Generation and reactions of the chlorine atom in aqueous solution. *J. Chem. Soc., Faraday Trans. 1* **1988**, *84* (10), 3319−3330.
(42) Balci, B.; Oturan, N.; Cherrier, R.; Oturan, M. A. Degradation of atrazine in aqueous medium by electrocatalytically generated hydroxyl radicals. A kinetic and mechanistic study. *Water Res.* **2009**, *43* (7), 1924−1934.
(43) Malpass, G. R. P.; Miwa, D. W.; Machado, S. A. S.; Olivi, P.; Motheo, A. J. Oxidation of the pesticide atrazine at DSA (R) electrodes. *J. Hazard. Mater.* **2006**, *137* (1), 565−572.
(44) Oturan, N.; Brillas, E.; Oturan, M. A. Unprecedented total mineralization of atrazine and cyanuric acid by anodic oxidation and electro-Fenton with a boron-doped diamond anode. *Environ. Chem. Lett.* **2012**, *10* (2), 165−170.
(45) De Battisti, A.; Ferro, S.; Dal Colle, M. Electrocatalysis at conductive diamond modified by noble-metal oxides. *J. Phys. Chem. B* **2001**, *105* (9), 1679−1682.
(46) Kumar, K.; Margerum, D. W. Kinetics and mechanisms of general acid assisted oxidation of bromide by hypochlorite and hypochlorous acid. *Inorg. Chem.* **1987**, *26* (16), 2706−2711.
(47) Winid, B. Bromine and water quality − Selected aspects and future perspectives. *Appl. Geochem.* **2015**, *63*, 413−435.
(48) Warner, N. R.; Christie, C. A.; Jackson, R. B.; Vengosh, A. Impacts of Shale Gas Wastewater Disposal on Water Quality in Western Pennsylvania. *Environ. Sci. Technol.* **2013**, *47* (20), 11849−11857.
(49) Ferro, S.; Battisti, A. D. The Bromine Electrode. Part I: Adsorption Phenomena at Polycrystalline Platinum Electrodes. *J. Appl. Electrochem.* **2004**, *34* (10), 981−987.
(50) Ferro, S.; Orsan, C.; De Battisti, A. The bromine electrode Part II: reaction kinetics at polycrystalline Pt. *J. Appl. Electrochem.* **2005**, *35* (3), 273−278.
(51) Pinkston, K. E.; Sedlak, D. L. Transformation of aromatic ether- and amine-containing pharmaceuticals during chlorine disinfection. *Environ. Sci. Technol.* **2004**, *38* (14), 4019−4025.
(52) Dodd, M. C.; Huang, C. H. Aqueous chlorination of the antibacterial agent trimethoprim: Reaction kinetics and pathways. *Water Res.* **2007**, *41* (3), 647−655.
(53) Dodd, M. C.; Huang, C.-H. Transformation of the Antibacterial Agent Sulfamethoxazole in Reactions with Chlorine: Kinetics, Mechanisms, and Pathways. *Environ. Sci. Technol.* **2004**, *38* (21), 5607−5615.
(54) Huang, L.; Li, L.; Dong, W.; Liu, Y.; Hou, H. Removal of Ammonia by OH Radical in Aqueous Phase. *Environ. Sci. Technol.* **2008**, *42* (21), 8070−8075.
(55) Neta, P.; Maruthamuthu, P.; Carton, P. M.; Fessenden, R. W. Formation and reactivity of the amino radical. *J. Phys. Chem.* **1978**, *82* (17), 1875−1878.
(56) Giguère, P. A.; Herman, K. A remarkably long-lived radical: The aminoperoxy, NH_2O_2. *Chem. Phys. Lett.* **1976**, *44* (2), 273−276.
(57) Dodd, M. C.; Zuleeg, S.; von Gunten, U.; Pronk, W. Ozonation of Source-Separated Urine for Resource Recovery and Waste Minimization: Process Modeling, Reaction Chemistry, and Operational Considerations. *Environ. Sci. Technol.* **2008**, *42* (24), 9329−9337.
(58) Wenk, J.; von Gunten, U.; Canonica, S. Effect of Dissolved Organic Matter on the Transformation of Contaminants Induced by Excited Triplet States and the Hydroxyl Radical. *Environ. Sci. Technol.* **2011**, *45* (4), 1334−1340.
(59) Wenk, J.; Canonica, S. Phenolic Antioxidants Inhibit the Triplet-Induced Transformation of Anilines and Sulfonamide Antibiotics in Aqueous Solution. *Environ. Sci. Technol.* **2012**, *46* (10), 5455−5462.
(60) Wenk, J.; Aeschbacher, M.; Salhi, E.; Canonica, S.; von Gunten, U.; Sander, M. Chemical Oxidation of Dissolved Organic Matter by Chlorine Dioxide, Chlorine, And Ozone: Effects on Its Optical and Antioxidant Properties. *Environ. Sci. Technol.* **2013**, *47* (19), 11147−11156.
(61) Appiani, E.; Page, S. E.; McNeill, K. On the Use of Hydroxyl Radical Kinetics to Assess the Number-Average Molecular Weight of

DOI: 10.1021/acs.est.6b02232
Environ. Sci. Technol. XXXX, XXX, XXX−XXX

Dissolved Organic Matter. *Environ. Sci. Technol.* **2014**, *48* (20), 11794−11802.
(62) Kim, C.; Kim, S.; Choi, J.; Lee, J.; Kang, J. S.; Sung, Y. E.; Lee, J.; Choi, W.; Yoon, J. Blue TiO_2 Nanotube Array as an Oxidant Generating Novel Anode Material Fabricated by Simple Cathodic Polarization. *Electrochim. Acta* **2014**, *141*, 113−119.
(63) Barazesh, J. M.; Hennebel, T.; Jasper, J. T.; Sedlak, D. L. Modular Advanced Oxidation Process Enabled by Cathodic Hydrogen Peroxide Production. *Environ. Sci. Technol.* **2015**, *49* (12), 7391−7399.
(64) Neta, P.; Huie, R. E.; Ross, A. B. Rate constants for reactions of inorganic radicals in aqueous solution. *J. Phys. Chem. Ref. Data* **1988**, *17* (3), 1027−1284.
(65) Deborde, M.; von Gunten, U. Reactions of chlorine with inorganic and organic compounds during water treatment - Kinetics and mechanisms: A critical review. *Water Res.* **2008**, *42* (1−2), 13−51.
(66) Kostich, M. S.; Batt, A. L.; Lazorchak, J. M. Concentrations of prioritized pharmaceuticals in effluents from 50 large wastewater treatment plants in the US and implications for risk estimation. *Environ. Pollut.* **2014**, *184*, 354−359.
(67) Solomon, K. R.; Baker, D. B.; Richards, R. P.; Dixon, D. R.; Klaine, S. J.; LaPoint, T. W.; Kendall, R. J.; Weisskopf, C. P.; Giddings, J. M.; Giesy, J. P.; Hall, L. W.; Williams, W. M. Ecological risk assessment of atrazine in North American surface waters. *Environ. Toxicol. Chem.* **1996**, *15* (1), 31−74.
(68) Bergmann, M. E. H.; Koparal, A. S.; Iourtchouk, T. Electrochemical Advanced Oxidation Processes, Formation of Halogenate and Perhalogenate Species: A Critical Review. *Crit. Rev. Environ. Sci. Technol.* **2014**, *44* (4), 348−390.
(69) Farhat, A.; Keller, J.; Tait, S.; Radjenovic, J. Removal of Persistent Organic Contaminants by Electrochemically Activated Sulfate. *Environ. Sci. Technol.* **2015**, *49* (24), 14326−14333.

DOI: 10.1021/acs.est.6b02232
Environ. Sci. Technol. XXXX, XXX, XXX−XXX